

Low energy chiral two pion exchange potential with statistical uncertainties

R. Navarro Pérez,^{1,2,*} J.E. Amaro,^{1,†} and E. Ruiz Arriola^{1,‡}

¹*Departamento de Física Atómica, Molecular y Nuclear and Instituto Carlos I de Física Teórica y Computacional
Universidad de Granada, E-18071 Granada, Spain.*

²*Department of Physics and Astronomy, Iowa State University, Ames, Iowa 50011, USA.*
(Dated: November 6, 2014)

We present a new phenomenological Nucleon-Nucleon chiral potential fitted to 925 pp and 1743 np scattering data up to a laboratory energy of 125 MeV with 20 short distance parameters and three chiral constants c_1 , c_3 and c_4 with $\chi^2/\nu = 1.02$. Special attention is given to testing the normality of the residuals which allows for a sound propagation of statistical errors from the experimental data to the potential parameters, phase-shifts, scattering amplitudes and counter-terms. This fit allows for a new determination of the chiral constants c_1 , c_3 and c_4 compatible with previous determinations from NN data. We further explore the interplay between the error analysis and the assumed form of the short distance interaction. The present work shows that it is possible to fit NN scattering with a TPE chiral potential fulfilling all necessary statistical requirements up to 125 MeV and shows unequivocal non-vanishing D-wave short distance pieces.

PACS numbers: 03.65.Nk, 11.10.Gh, 13.75.Cs, 21.30.Fe, 21.45.+v

Keywords: NN interaction, Two Pion Exchange, Statistical Analysis, Chiral interaction

I. INTRODUCTION

The NN interaction is beyond any doubt a key building block of nuclear physics but, what are the decisive features which make the interaction qualify for an *ab initio* description of binding in nuclei ?

From a statistical point of view, a traditional figure of merit has been the value of χ^2/ν after a least squares minimization fit np and pp scattering data with $\nu = N - P$, the difference between the number of fitted data and the number of fitting parameters. This approach was initiated in 1957 at about pion production threshold energies [1] (see [2, 3] for reviews) and extended up to 3GeV more recently with a $\chi^2/\nu \sim 1.4$ [4]. After the benchmarking Partial Wave Analysis (PWA) of the Nijmegen group 20 years ago [5, 6], the path and key necessary features were shown to provide a statistically satisfactory fit, i.e. having an expected $\chi^2_{\min}/\nu \sim 1 \pm \sqrt{2/\nu}$ within 1σ confidence level up to about pion production threshold: suitable data selection, incorporating charge dependent One Pion Exchange (OPE) interactions as well as many EM features and an adequate statistical interpretation of results [7, 8]. This χ^2/ν -values have set the standards in high quality NN studies [6, 9–15]. The least squares χ^2 -fit approach uses selected experimental data with uncertainties which should be described in terms of a postulated theory according to accepted statistical principles. In particular, if the theory is flexible enough the difference between the actual measured data and the proposed theory should be a statistical fluctuation. The size of the fluctuation is controlled by the number of available data as well the reported experimental uncertainties. This is the essence of the normality test for residuals which relevance we have recently stressed [15, 16] (see Refs. [7, 8]

for related ideas). The main advantage is that if this test is passed correctly we expect the addition of new data in the future to sharpen the estimates of the theoretical parameters.

The standard choice of pion-production threshold as upper limit at CM momentum $p \sim \sqrt{M_N m_\pi} \sim 360\text{MeV}$ is essentially based on the simplicity of treatment, as one may ignore the explicit contribution of the inelastic $NN \rightarrow NN\pi$ channel, but it does not tell anything on the shortest physical length scale operating in the binding of finite nuclei. Fortunately, even for nuclear matter characterized by the Fermi momentum $p_F \sim 250\text{MeV}$ the role of these inelasticities is negligible since $p_F \lesssim \sqrt{M_N m_\pi}$, and thus one may reduce the upper fitting energy, the more the lighter the nucleus. Afnan and Tang recognized this for the case of ${}^3\text{He}$ and ${}^4\text{He}$ [17] where good binding energies were achieved when S-waves are fitted up to $E_{\text{LAB}} \lesssim 100\text{MeV}$. Using simple coarse grained interactions and mean field wave functions we have verified this feature for nuclei as heavy as ${}^{40}\text{Ca}$ [18].

On the hadronic scale, finite nuclei are weakly bound objects of neutrons and protons and thus their de Broglie wavelength is large enough for them to behave effectively as elementary particles. On the other hand, when nucleons are far apart, say $r \gtrsim 2\text{fm}$, they do not to overlap and their interaction resembles a van der Waals type of exchange of pions between point like nucleons (see e.g. [19, 20] for a quark cluster point of view). In such a case the corresponding scattering partial wave amplitudes containing $n - \pi$ exchanges are analytical in the complex CM-momentum plane at $p = \pm im_\pi/2$. This provides upper limits in the maximal energy on the number of exchanged pions which should be taken into account to represent the scattering amplitude with the correct analytical structure. At pion production threshold this gives $n \sim 2\sqrt{M_N/m_\pi} \sim 5$ pion exchanges, which seems almost impossible to implement. In practice, the strength of the discontinuity of the scattering amplitude may be small enough to relax this requirement.

From the point of view of Quantum Chromo-Dynamics (QCD) hadronic interactions can be described with sub-

*Electronic address: nnavarrop@ugr.es

†Electronic address: amaro@ugr.es

‡Electronic address: earriola@ugr.es

nuclear degrees of freedom like quarks and gluons and lattice calculations for NN potentials have been pursued in terms of these fundamental degrees of freedom [21, 22]. On the other hand, the spontaneous breaking of chiral symmetry allows to derive a NN interaction with multiple pion exchange for the long range part in terms of an effective low energy Lagrangian where pions enter via derivative couplings of the field $\sim \partial\Phi/f_\pi \sim p/f_\pi\Phi$ with $f_\pi = 92\text{MeV}$ the pion weak decay constant [23–25]. Actually, the breakdown scale Λ_χ for a theory with just pions and nucleons is expected to be at the branch cut $\Lambda_\chi \sim |p| = m_R/2$ corresponding to pionic resonance exchanges. A large N_c quark-hadron duality argument gives $m_\rho \sim \sqrt{24\pi/N_c}f_\pi$ [26] and more complete treatments yield indeed similar estimates for m_R with $R = \rho, A_1, \pi^*, \sigma$ [27]. Therefore the strength of the discontinuity of the scattering amplitude due to chiral $n\pi$ exchange is suppressed as $(m_\pi n/(2\Lambda_\chi))^{2n}$. Thus, from the point of view of the operationally *needed* and the theoretically *available* higher scale the consideration of chiral TPE seems like a perfect match up to $p \lesssim 3m_\pi/2$ corresponding to the location of 3π -exchange cut and a LAB energy of $T_{\text{LAB}} \sim 90\text{MeV}$.

This type of chiral effective interactions can be implemented as standard quantum mechanical potentials expanded in powers of momentum relative to Λ_χ and still require the use of phenomenological counter-terms featuring the integrated out short distance behavior. Thus, a comparison of chiral potentials to NN scattering data is indispensable, even at very low energies [28–31]. Since the mid-nineties several interactions, at different orders, have been developed attempting to accurately describe NN scattering processes with chiral components as their main feature. In recent years a trend to compromise the description of intermediate and high energy data in exchange for a more accurate representation of low energy data, $E_{\text{LAB}} \lesssim 125\text{MeV}$, has emerged [32–35]. The non-trivial question is whether this theoretical expectation is confirmed by the statistical analysis of the currently available data below those energies.

Moreover, this reduction in the fitted energy range implies a trade-off between improved theoretical reliability and a loss of many scattering data in the analysis. This may also imply a loss of precision and, as a consequence, a loss of predictive power [36]. This paper studies this interplay between precision and predictive power by fitting a chiral potential to low energy data, $E_{\text{LAB}} \lesssim 125\text{MeV}$ and undertaking the statistical uncertainties.

Using a Delta-Shell (DS) potential initially proposed by Avilés [37] and rediscovered in Ref. [38] it was possible to coarse grain the NN interaction by proving it at certain sensible points [18, 39]. To select a self-consistent data base of over 6700 scattering data up to laboratory energy of 350MeV we fitted a DS potential with a one pion exchange (OPE) potential tail starting at 3.0 fm and electromagnetic EM effects [12, 13]. Once the data base was fixed we modified the DS potential including a chiral two pion exchange χ TPE tail starting at 1.8fm and made a new determination of the chiral constants c_1, c_3 and c_4 with statistical uncertainties [14]. Also a local and smooth potential, that describes the same database [15], has allowed to propagate statistical uncertain-

ties into few body calculations [40]. The basic requirement of normally distributed data for any least squares fit is verified; it has been checked for all three phenomenological potentials previously mentioned [15].

In this work we present a new DS- χ TPE potential fitted to low energy data up to 125MeV LAB energy. This has practical advantages as the core gets reduced improving on the suitability of mean field schemes [18] because the effective interaction evolves with this upper fitted energy [41]. We have also previously reported on the consequences of reducing the upper limit [36] and how the statistical uncertainties of phase-shifts and shell model matrix elements increase to the point of making OPE and χ TPE indistinguishable. This would be a situation where the only advantage of χ TPE over OPE would be in the reduction of the number of parameters, but not so much in a better quality in the description of the data.

Finally, we hasten to emphasize that ours is *not* a conventional χ PT calculation; we use long range potentials above a certain distance r_c and coarse grain the short part of the interaction below that distance with a sampling $\Delta r \sim \hbar/p_{\text{max}}$ resolution [42], but take no position on how the short distance piece should be organized within a perturbative setup. In this regard, let us mention that while there is agreement on the long distance features of multi-pionic exchange interactions based on χ PT, much has been said on the way the short distance pieces of the interaction should be organized. The discussion on the specific power counting to be applied within χ PT has been around since the very beginning and most discussions have been carried out on the basis of theoretical consistency [43–45]. To date these alternative schemes have not been seriously confronted to experimental np and pp scattering data *directly* as we do here by using the classical statistical χ^2 least squares approach.

The paper is organized as follows. In Section II we present our potential and the necessary details for the fit, the normality issues and error propagation. In Section III we generate scattering properties including phase shifts, scattering amplitudes and low energy threshold parameters. The low momentum structure of the theory is presented and discussed in Section IV. In Section V we analyze other existing approaches in the literature and discuss in detail their statistical features. Finally, in Section VI we come to our main conclusions.

II. COARSE GRAINED POTENTIAL

For a motivation on the use of a coarse grained potential in nuclear physics we refer to Ref. [18]. The anatomy of the NN potential including multi-pion exchange and the expected number of fitted parameters has been discussed in Ref. [42].

A. Form of the potential

The structure of the potential is the same as the DS- χ TPE potential of [14] with a clear boundary $r_c = 1.8\text{fm}$ between the short range phenomenological part with delta-shells and

the long range tail with one and two pion exchange plus electromagnetic interactions.

$$V(r) = V_{\text{DS}}(r) + [V_{\text{OPE}}(r) + V_{\text{TPE}}(r) + V_{\text{EM}}]\theta(r - r_c). \quad (1)$$

The long range potentials are the same as the ones used in [14], although the chiral constants c_1 , c_3 and c_4 in $V_{\text{TPE}}(r)$ are used as fitting parameters. The DS part is given by

$$V_{\text{DS}} = \sum_{n=1}^{21} O_n \left[\sum_{i=1}^N V_{i,n} \Delta r \delta(r - r_i) \right], \quad r \leq r_c \quad (2)$$

where O_n is the set of operators in the extended AV18 basis detailed in Appendix A of [13], $V_{i,n}$ are strength coefficients, r_i are the concentration radii and $\Delta r = 0.6\text{fm}$ is the distance between them. As with previous works we decompose the potential into partial waves by

$$V_{l,l'}^{J,S}(r) = \frac{1}{2\mu_{\alpha\beta}} \sum_{i=1}^N (\lambda_i)^{S,J} \delta(r - r_i), \quad r \leq r_c \quad (3)$$

and use the 15 lowest angular momentum partial waves to parameterize the full potential and calculate the more peripheral partial waves by decomposing back from the operator basis to the partial wave basis.

The choice above is based on the high quality of our previous fit up to $T_{\text{LAB}} = 350\text{MeV}$ which fulfills all needed statistical tests (see below). Our aim is that by reducing the energy range to $T_{\text{LAB}} = 125\text{MeV}$ correlations among the parameters will appear implying a reduction of the number of independent parameters. Although the error of the data below $T_{\text{LAB}} = 125\text{MeV}$ is the same, their induced propagation is amplified as a result of a fitting a smaller number of data. Even the observables computed below 125MeV exhibit a larger error.

B. Fitting short distance parameters

Below $T_{\text{LAB}} \leq 125\text{MeV}$ the self-consistent data base obtained in [13] contains $N_{pp} = 925$ pp data and $N_{np} = 1743$ np data including normalizations. This upper limit on the laboratory frame energy allows to reduce the number of parameters from 30 in [14] to 20, apart from the 3 chiral constants. Of course, with less data constraining the interaction the statistical uncertainties in the potential parameters are larger. The resulting delta-shell fitting parameters yield a total value of $\chi^2/\nu = 1.02$ and are shown in Table I. Note that to 1σ confidence level, one expects $\chi^2/\nu = 1 \pm \sqrt{2/\nu}$, which in this particular case means $0.097 \leq \chi^2/\nu \leq 1.03$.

This fit provides a new determination of the chiral constants $c_1 = -0.27 \pm 2.87$, $c_3 = -5.77 \pm 1.58$ and $c_4 = 4.24 \pm 0.73 \text{ GeV}^{-1}$ which is mostly compatible to the one from [14]. In Figure 1 we compare the ellipses of the present fit with those of our previous fit to 350 MeV [14]. Although each individual constant, with its corresponding 1σ confidence interval, is statistically compatible with the determination with data up to $T_{\text{LAB}} = 350 \text{ MeV}$, the correlation ellipses of both fits for the c_1, c_3 pair do not overlap.

TABLE I: Delta-shell parameters fitted to reproduce 2668 pp and np scattering data with $T_{\text{LAB}} \leq 125\text{MeV}$. Statistical error bars are propagated from experimental uncertainties. The complete potential has a $\chi^2\text{TPE}$ tail for $r > 1.8\text{fm}$ and all relevant electromagnetic interactions.

Wave	λ_1	λ_2	λ_3
	($r_1 = 0.6\text{fm}$)	($r_1 = 1.2\text{fm}$)	($r_1 = 1.8\text{fm}$)
^1S_0np	0.88(79)	-0.75(19)	-0.053(46)
^1S_0pp	1.9(2)	-0.89(3)	-0.028(9)
3P_0	-	0.40(13)	-0.061(26)
1P_1	-	1.06(9)	-
3P_1	-	1.5(1)	0.016(13)
3S_1	1.6(6)	-	-
ϵ_1	-	-2.78(8)	-0.19(4)
3D_1	-	3.0(5)	-
1D_2	-	-0.58(7)	-
3D_2	-	-	-0.28(1)
3P_2	-	-0.44(1)	-
ϵ_2	-	-	0.097(11)
3F_2	-	-	-
1F_3	-	-	-
3D_3	-	1.1(1)	-

C. Normality test

Once the potential parameters are fitted to the self-consistent data base we check the normality of the residuals

$$R_i = \frac{O_i^{\text{exp}} - O_i^{\text{theo}}}{\Delta O_i^{\text{exp}}}. \quad (4)$$

To this end we apply the recently introduced Tail-Sensitive (TS) test [46]. The TS test compares the quantiles of an empirical distribution with the quantiles of a normal distribution. The finite size of the sample gives a confidence interval for each quantile which can be calculated analytically for a previously determined significance level. If an empirical quantile falls outside of its corresponding confidence interval the hypothesis of normality is rejected. In figure 2 we show a rotated quantile-quantile (QQ) plot comparing the theoretical quantiles of the standard normal distribution $N(0, 1)$ with the residuals quantiles; the confidence intervals for the TS and the more familiar Kolmogorov-Smirnov (KS) tests are also shown with a significance level $\alpha = 0.05$. As can be seen, the empirical residuals resulting for the low energy fit always fall within the 95% confidence bands of both the TS and KS normality tests.

Aside from obtaining a graphical representation, testing for normality is a straightforward procedure which simply requires to calculate a quantity known as a test statistic T and compare it with a previously tabulated (or parameterized) critical value T_c as a function of the sample size N . Depending on the definition of T on each normality test, a larger (or conversely, smaller) T indicates larger deviations from the normal distribution and $T > T_c$ (or $T < T_c$) gives significant evidence to reject the hypothesis of normality; in the particular case of the TS test large deviations from the normal distribution result in small values for T . For the TS test a recipe for cal-

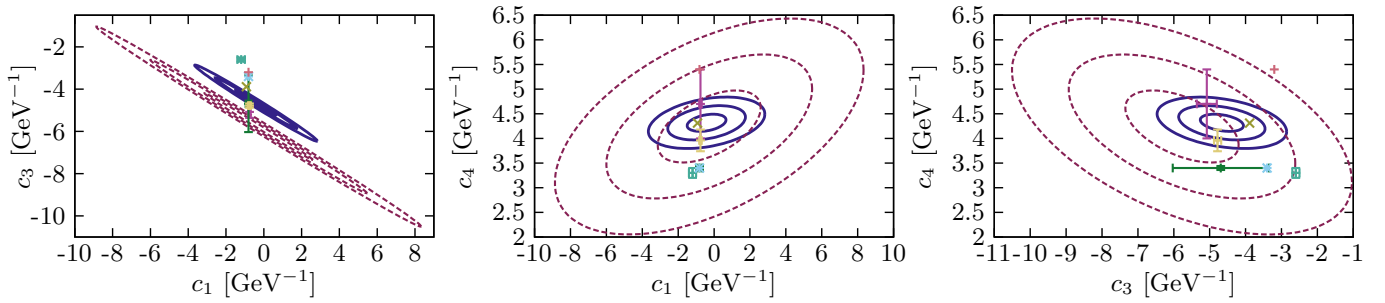


FIG. 1: (Color online) Correlation ellipses of the chiral constants c_1 , c_3 and c_4 determined from a fit to the self consistent database of [13] with a DS- χ TPE potential including data with $T_{\text{LAB}} \leq 350$ [14] (blue solid lines) and $T_{\text{LAB}} \leq 125$ (red dashed lines). The concentric ellipses give, from the smallest to the largest one, the 68%, 95% and 99% confidence regions respectively. The points and crosses correspond to the determinations listed in Table VI of [14]

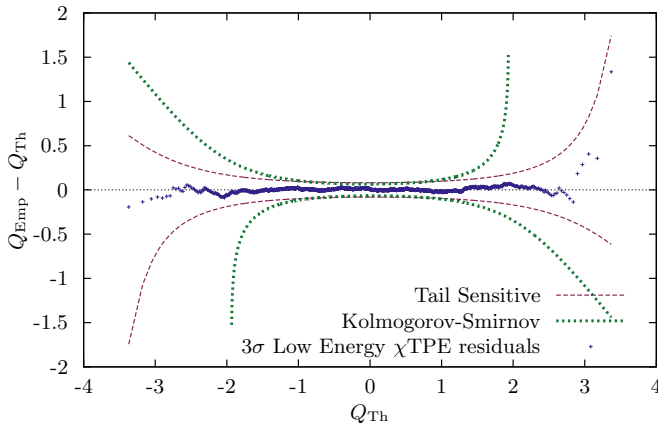


FIG. 2: (Color online) Rotated quantile-quantile plot for the residuals of the low energy DS- χ TPE potential for $E_{\text{LAB}} \leq 125$ MeV (blue crosses). The Kolmogorov-Smirnov (dotted green line) and Tail sensitive (dashed red line) confidence bands with an $\alpha = 0.05$ significance level are also included.

culating T , a table of T_c for $N \leq 50$ and a parameterization for $50 < N < 9000$ can be found in [16]. The residuals of the low energy fit to the self consistent database give $T = 0.0068$ and the critical value for a sample size $N = 2668$ and a significance level $\alpha = 0.05$ is $T_c = 0.0008$ and therefore there is not significant evidence to reject the normality of the residuals.

D. Error propagation

Once the normality test is passed, we may proceed to propagate the errors inherited by the theory through the χ^2 -fit. We do so below for the phase shifts, the full scattering amplitude and the low energy threshold parameters. Several schemes are possible [47]: i) the standard covariance matrix of building derivatives in quadrature with correlations, ii) the Monte Carlo method based on a multivariate gaussian distribution based on the χ^2 function, and iii) the more elaborated bootstrap method [47]. Results are fairly similar in all three cases and we use for definiteness the method ii).

III. SCATTERING PROPERTIES

A. Phase-shifts

In Figure 3 we show the low angular momentum partial wave phase-shifts up to $T_{\text{LAB}} = 350$ MeV for the low energy DS- χ TPE and the DS- χ TPE potential of [14]. The low energy version of the potential shows larger statistical uncertainties at higher energies since there are no data constraining the interaction above 125 MeV. However, below this energy value statistical error bands are also larger for the low energy version of the potential. This indicates that the high energy data also play a significant role in determining the uncertainties at lower energies.

B. Wolfenstein parameters

The full NN scattering amplitude reads

$$M = a + m(\boldsymbol{\sigma}_1 \cdot \mathbf{n})(\boldsymbol{\sigma}_2 \cdot \mathbf{n}) + (g - h)(\boldsymbol{\sigma}_1 \cdot \mathbf{m})(\boldsymbol{\sigma}_2 \cdot \mathbf{m}) + (g + h)(\boldsymbol{\sigma}_1 \cdot \mathbf{l})(\boldsymbol{\sigma}_2 \cdot \mathbf{l}) + c(\boldsymbol{\sigma}_1 + \boldsymbol{\sigma}_2) \cdot \mathbf{n} \quad (5)$$

where the Wolfenstein parameters a, m, g, h, c depend on energy and scattering angle, $\boldsymbol{\sigma}_1$ and $\boldsymbol{\sigma}_2$ are the single-nucleon Pauli matrices, $\mathbf{l}, \mathbf{m}, \mathbf{n}$ are three unitary orthogonal vectors along the directions of $\mathbf{k}_f + \mathbf{k}_i$, $\mathbf{k}_f - \mathbf{k}_i$ and $\mathbf{k}_i \wedge \mathbf{k}_f$, respectively, and $(\mathbf{k}_f, \mathbf{k}_i)$ are the final and initial relative nucleon momenta. The relation with the phase shifts can be looked up in Refs. [13, 48].

Figures 4, 5 and 6 compare the Wolfenstein parameters of the low energy DS- χ TPE potential with the full DS- χ TPE ones at 50, 100 and 200 MeV respectively. At lower energies both interactions show a fair level of agreement and again the low energy version of the potential shows larger uncertainties. At 200 MeV the discrepancies are much larger, however this is beyond the range of validity of this new interaction.

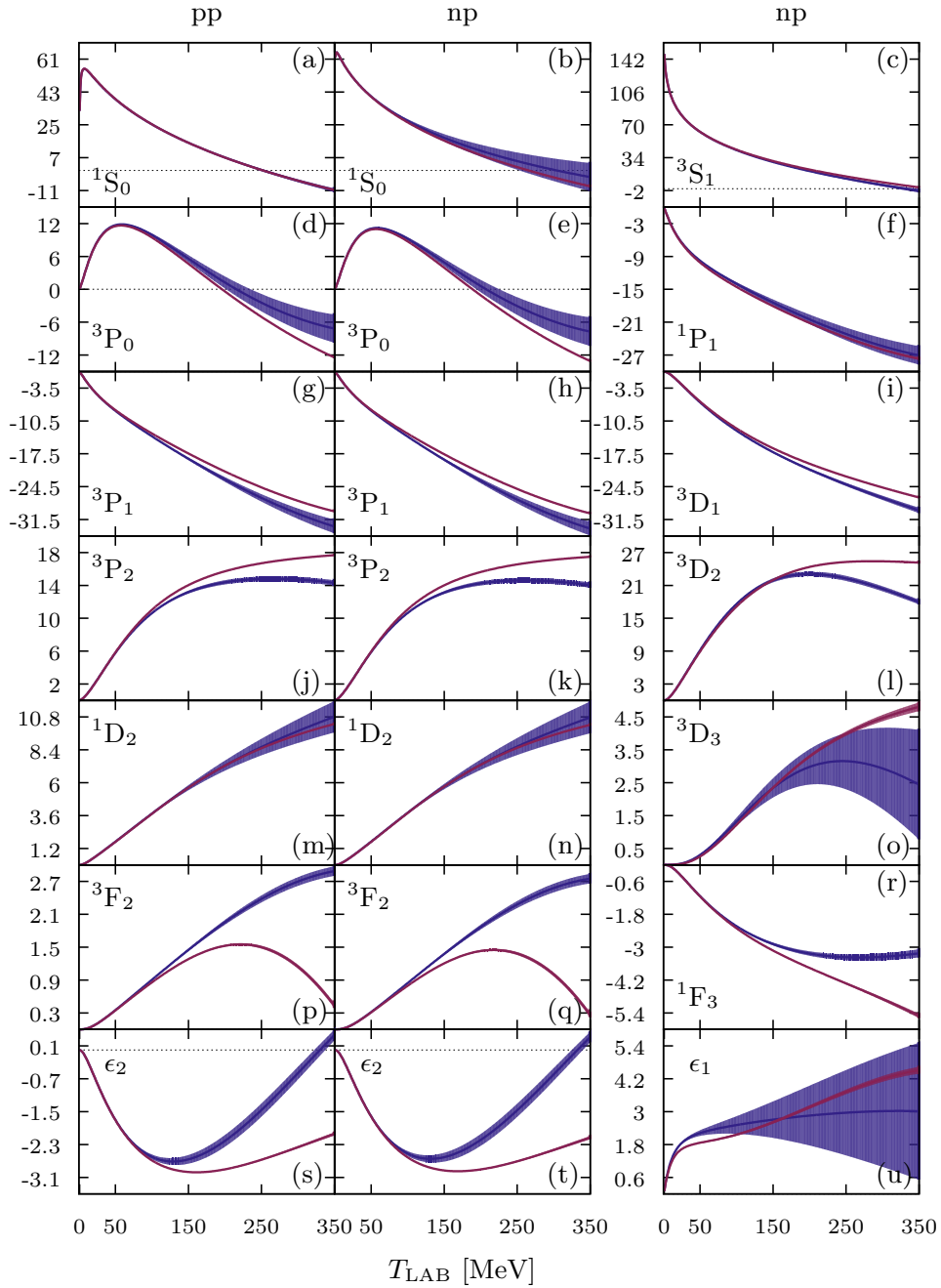


FIG. 3: (Color online) Phase-shifts for the low energy DS- χ TPE potential fitted to experimental data with $T_{\text{LAB}} \leq 125\text{MeV}$ with statistical error bands (blue bands). The corresponding phase-shifts and error bands for the full DS- χ TPE reproducing data with $T_{\text{LAB}} \leq 350\text{ MeV}$ [14] are also included for comparison (red bands)

C. Low energy threshold parameters

In the absence of tensor force the phase-shifts with angular momentum l behave for low CM momentum, $k \rightarrow 0$, according to the effective range expansion

$$k^{2l+1} \cot \delta_l(k) = -\frac{1}{\alpha_l} + \frac{1}{2}r_l k^2 + v_{2,l}k^4 + \dots, \quad (6)$$

When the tensor force is considered we can apply a coupled channel generalization of the effective range expansion [49].

Introducing the $\hat{\mathbf{M}}$ matrix defined as

$$\mathbf{DSD}^{-1} = (\hat{\mathbf{M}} + ik\mathbf{D}^2)(\hat{\mathbf{M}} - ik\mathbf{D}^2)^{-1}, \quad (7)$$

where \mathbf{S} is the usual unitary S-matrix and $\mathbf{D} = \text{diag}(k^{l_1}, \dots, k^{l_N})$. In the limit $k \rightarrow 0$, the $\hat{\mathbf{M}}$ -matrix becomes

$$\hat{\mathbf{M}} = -\mathbf{a}^{-1} + \frac{1}{2}\mathbf{r}k^2 + \mathbf{v}_2k^4 + \mathbf{v}_3k^6 + \mathbf{v}_4k^8 + \dots, \quad (8)$$

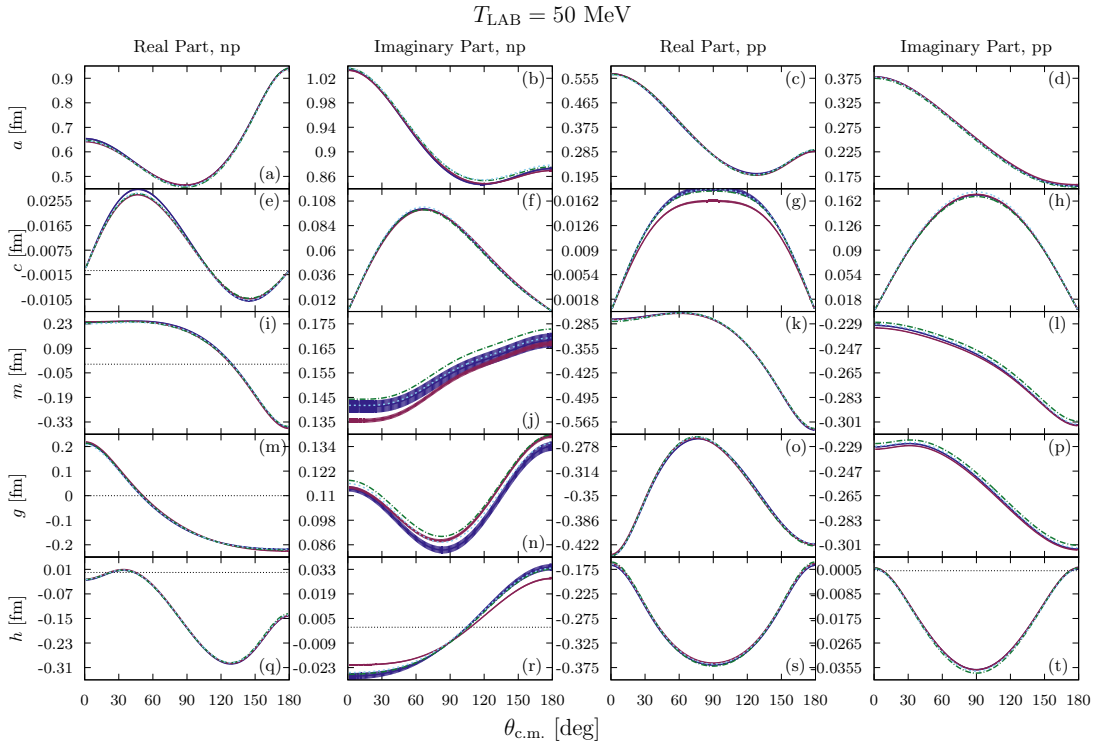


FIG. 4: (Color online) np (left) and pp (right) Wolfenstein parameters (in fm) as a function of the c.m. angle (in degrees) and for $T_{\text{LAB}} = 50 \text{ MeV}$. We compare the low energy DS- χ TPE potential (blue band) with full DS- χ TPE potential [14] (red band) the Nijmegen PWA [5] (dotted, light blue line) and the AV18 potential [9] (dashed-dotted, green line).

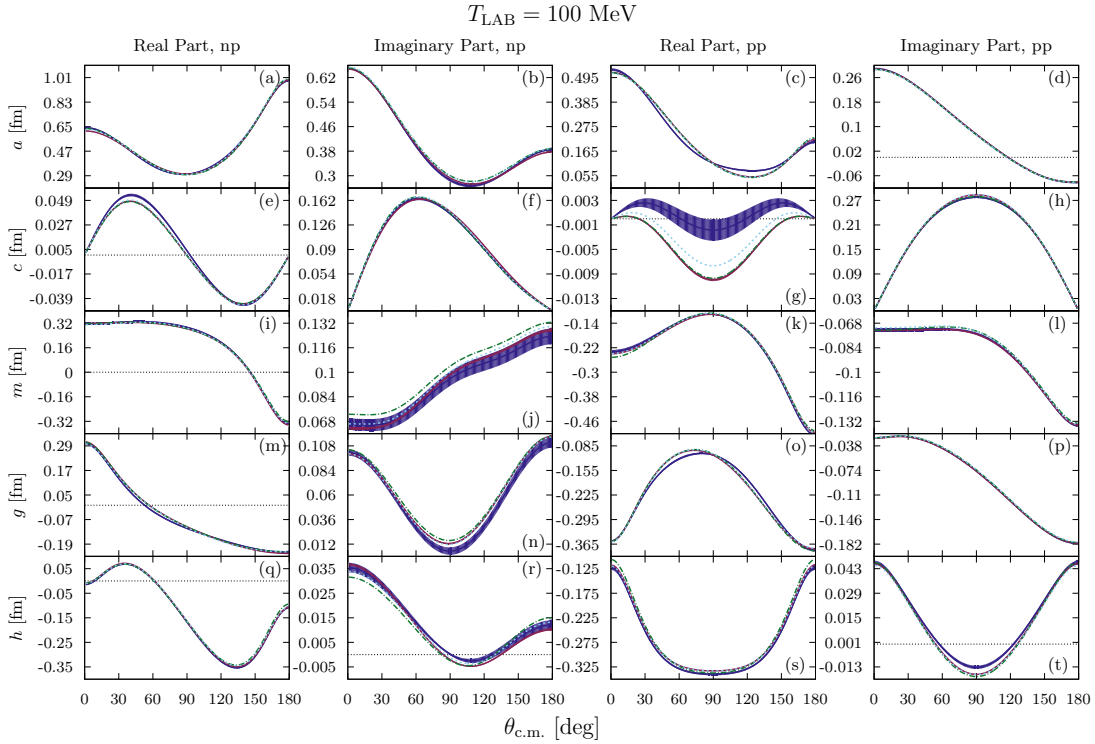


FIG. 5: (Color online) Same as Fig. 4 but for $T_{\text{LAB}} = 100 \text{ MeV}$

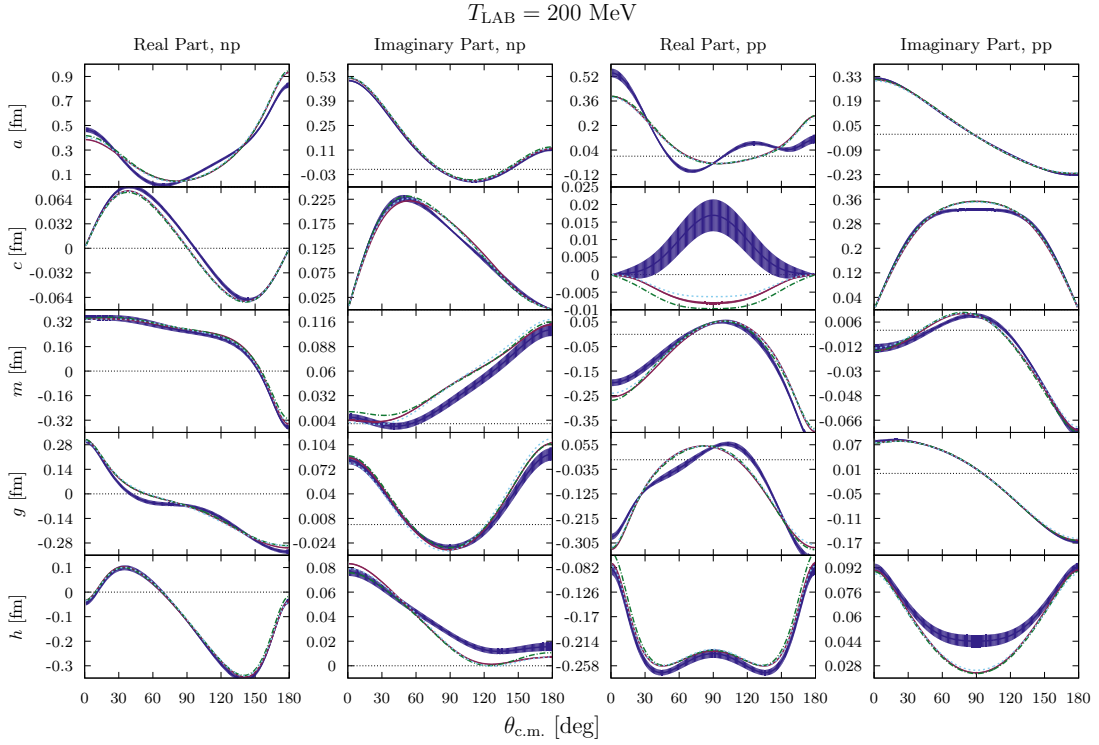


FIG. 6: (Color online) Same as Fig. 4 but for $T_{\text{LAB}} = 200 \text{ MeV}$

where \mathbf{a} , \mathbf{r} and \mathbf{v}_i are the coupled channel generalizations of α_0 , r_0 and v_i respectively. We have recently evaluated them and confronted statistical and systematic errors based on this expansion [50].

Table II shows the low energy threshold parameters of all partial waves with $j \leq 5$ for the low energy DS- χ TPE potential. The statistical uncertainties are propagated by drawing 1000 random sets of potential parameters following a multivariate normal distribution according to the covariance matrix, calculating the low energy threshold parameters for each set of parameters and taking the mean and standard deviation.

IV. EFFECTIVE INTERACTIONS AT LOW MOMENTUM

We now turn to analyze the corresponding potential in momentum space, particularly within a low momentum expansion. As we have shown elsewhere [41], the coefficients of the expansion can be mapped into radial moments of volume integrals of the potential, which exhibit some degree of universality. We will separate the contributions stemming from the inner region $r < r_c$ containing just delta-shell interactions and the outer region $r > r_c$ containing the pion exchange potential tail. For ease of comparison, we will consider the results in a Cartesian as well as in the spherical basis.

A. Moshinsky-Skyrme parameters

At the two body level the effective interaction of Moshinsky [51] and Skyrme [52] can be written as a pseudo-potential in the form

$$\begin{aligned}
 V_{\Lambda}(\mathbf{p}', \mathbf{p}) &= \int d^3x e^{-i\mathbf{x} \cdot (\mathbf{p}' - \mathbf{p})} \hat{V}(\mathbf{x}) \\
 &= t_0(1 + x_0 P_{\sigma}) + \frac{t_1}{2}(1 + x_1 P_{\sigma})(\mathbf{p}'^2 + \mathbf{p}^2) \\
 &\quad + t_2(1 + x_2 P_{\sigma})\mathbf{p}' \cdot \mathbf{p} + 2iW_0 \mathbf{S} \cdot (\mathbf{p}' \wedge \mathbf{p}) \\
 &\quad + \frac{t_T}{2} \left[\sigma_1 \cdot \mathbf{p} \sigma_2 \cdot \mathbf{p} + \sigma_1 \cdot \mathbf{p}' \sigma_2 \cdot \mathbf{p}' - \frac{1}{3} \sigma_1 \cdot \sigma_2 (\mathbf{p}'^2 + \mathbf{p}^2) \right] \\
 &\quad + \frac{t_U}{2} \left[\sigma_1 \cdot \mathbf{p} \sigma_2 \cdot \mathbf{p}' + \sigma_1 \cdot \mathbf{p}' \sigma_2 \cdot \mathbf{p} - \frac{2}{3} \sigma_1 \cdot \sigma_2 \mathbf{p}' \cdot \mathbf{p} \right] + \mathcal{O}(p^4)
 \end{aligned} \tag{9}$$

where $P_{\sigma} = (1 + \sigma_1 \cdot \sigma_2)/2$ is the spin exchange operator with $P_{\sigma} = -1$ for spin singlet ($S = 0$), and $P_{\sigma} = 1$ for spin triplet ($S = 1$) states.

The effective interaction representation in terms of Moshinsky-Skyrme parameters are presented in tables III. Since both parameterizations consist of potential integrals, see Ref. [41], we show the contribution to the full parameter by the phenomenological short range part $r \leq r_c$ and the pion exchange tail $r > r_c$ with the corresponding uncertainties. Since the potential is determined by low energy data only, one would expect the short range contribution to counter-terms of the most peripheral partial waves to be compatible with zero. However, we see that although the errors are larger than those quoted in [16] for a DS- χ TPE potential fitted to data up to

TABLE II: Low energy threshold parameters for all partial waves with $j \leq 5$ for the DS- χ TPE potential. The central value and statistical error bars correspond to the mean and standard deviation of a population of 1000 parameters calculated with a Monte Carlo family of potential parameters drawn according to the covariance matrix of the potential parameters. For each partial wave we show the scattering length α , the effective range r_0 and the curvature parameters v_2 , v_3 and v_4 . For the coupled channels we use the nuclear bar parameterization of the S matrix. The units are in powers of femtometers determined by the orbital angular momentum quantum numbers l and l' of each partial wave

Wave	$\alpha(\text{fm}^{l+l'+1})$	$r_0(\text{fm}^{l+l'+1})$	$v_2(\text{fm}^{l+l'+3})$	$v_3(\text{fm}^{l+l'+5})$	$v_4(\text{fm}^{l+l'+7})$
1S_0	-23.739975 ± 0.019856	2.683075 ± 0.010688	-0.482309 ± 0.010963	3.876303 ± 0.043940	-19.536951 ± 0.122646
3P_0	-2.497645 ± 0.007007	3.809329 ± 0.017893	1.006610 ± 0.013141	3.861832 ± 0.044996	-7.889673 ± 0.083544
1P_1	2.780145 ± 0.008084	-6.461193 ± 0.029229	-1.707267 ± 0.050329	0.293702 ± 0.094128	7.970193 ± 0.083765
3P_1	1.514034 ± 0.002833	-8.667588 ± 0.022467	0.014268 ± 0.026836	-0.504544 ± 0.070704	-0.583288 ± 0.204727
3S_1	5.424721 ± 0.001887	1.833010 ± 0.003057	-0.120574 ± 0.002884	1.433963 ± 0.008492	-7.563664 ± 0.036475
ϵ_1	1.686135 ± 0.013563	0.426075 ± 0.006913	-0.243444 ± 0.010099	1.436825 ± 0.016457	-7.260537 ± 0.019671
3D_1	6.563492 ± 0.026034	-3.493365 ± 0.013119	-3.645026 ± 0.021307	1.135239 ± 0.017822	-2.638623 ± 0.020137
1D_2	-1.385117 ± 0.002580	14.895810 ± 0.045677	16.422846 ± 0.118270	-12.890261 ± 0.193378	37.903278 ± 0.601827
3D_2	-7.408744 ± 0.005410	2.851102 ± 0.003869	2.360846 ± 0.012195	-1.083437 ± 0.026133	1.753274 ± 0.026984
3P_2	-0.297390 ± 0.003170	-8.478863 ± 0.046753	-7.433750 ± 0.145525	-7.477923 ± 0.416712	-14.511322 ± 0.788810
ϵ_2	1.600387 ± 0.001190	-15.966142 ± 0.043977	-25.930128 ± 0.168760	-25.222196 ± 0.682425	-70.658514 ± 1.762290
3F_2	-0.974812 ± 0.001774	-5.957998 ± 0.058571	-24.133336 ± 0.209295	-83.161809 ± 0.899196	-124.079013 ± 3.081428
1F_3	8.377225 ± 0.002234	-3.925084 ± 0.001881	-9.873666 ± 0.010626	-15.298794 ± 0.056008	-2.050820 ± 0.129186
3F_3	2.680008 ± 0.001765	-10.037798 ± 0.011854	-20.952701 ± 0.056074	-20.389419 ± 0.257995	-30.275280 ± 0.643766
3D_3	-0.140354 ± 0.002730	1.371004 ± 0.000773	2.071825 ± 0.003553	1.913193 ± 0.013570	-0.549459 ± 0.019826
ϵ_3	-9.682379 ± 0.000465	3.260401 ± 0.000832	7.672521 ± 0.004167	9.579540 ± 0.019404	-1.135140 ± 0.047122
3G_3	4.874337 ± 0.000639	-0.030192 ± 0.001672	0.001640 ± 0.009409	-0.003425 ± 0.051735	-2.718540 ± 0.151814
1G_4	-3.212045 ± 0.000661	10.809086 ± 0.003870	34.473444 ± 0.024269	81.971319 ± 0.155640	104.049040 ± 0.521681
3G_4	-19.145092 ± 0.000743	2.058351 ± 0.000143	6.814736 ± 0.001002	16.772767 ± 0.007057	10.019825 ± 0.025122
3F_4	-0.016002 ± 0.001726	-3.053099 ± 0.002105	-4.815627 ± 0.012043	73.726022 ± 0.055466	664.426931 ± 0.126890
ϵ_4	3.585807 ± 0.000044	-9.548329 ± 0.002591	-37.136343 ± 0.014979	-185.113250 ± 0.061061	-587.360666 ± 0.413503
3H_4	-1.240294 ± 0.000290	-0.204717 ± 0.008206	-1.772049 ± 0.059293	-17.439098 ± 0.551235	-123.030299 ± 3.669909
1H_5	28.573515 ± 0.000317	-1.726914 ± 0.000034	-7.906396 ± 0.000320	-32.787619 ± 0.003254	-59.367511 ± 0.019300
3H_5	6.079919 ± 0.000281	-6.440909 ± 0.000514	-25.238708 ± 0.003801	-82.597219 ± 0.030382	-168.850963 ± 0.140866
3G_5	-0.009639 ± 0.000646	0.480549 ± 0.000017	1.878389 ± 0.000142	6.098743 ± 0.001302	6.785788 ± 0.006672
ϵ_5	-31.301936 ± 0.000033	1.556146 ± 0.000020	6.994315 ± 0.000180	28.175241 ± 0.001704	48.356412 ± 0.009264
3I_5	10.677985 ± 0.000110	0.010777 ± 0.000058	0.144456 ± 0.000542	1.427543 ± 0.005504	6.457572 ± 0.032654

TABLE III: Moshinsky-Skyrme parameters. We separate the contribution from the delta-shells short range parameters (corresponding to $r < r_c = 1.8\text{fm}$) and the χTPE potential tail (corresponding to $r > r_c$). Units are: t_0 in MeVfm^3 , t_1, t_2, W_0, t_U, t_T in MeVfm^5 , and x_0, x_1, x_2 are dimensionless.

	$r < r_c$	$r > r_c$	Full
t_0	-87.8(729)	-382.3(91)	-470.1(767)
x_0	-4.5(40)	-0.088(2)	-0.92(23)
t_1	77.2(98)	821.0(57)	898.1(117)
x_1	-1.2(1)	-0.00832(6)	-0.11(1)
t_2	243.1(195)	2212.5(159)	2455.6(113)
x_2	-0.58(4)	-0.911(2)	-0.877(3)
W_0	105.8(30)	4.7	110.5(30)
t_U	148.1(49)	1132.8(30)	1281.0(56)
t_T	-569.4(301)	-3836.0(90)	-4405.4(279)

350MeV, the short range counter-terms are never compatible with zero. It is also worth noting that the full integrals both for Moshinsky-Skyrme parameters and counter-terms show a large degree of universality when compared to the same parameters for the DS-OPE and DS- χTPE potentials shown in [16].

B. Counter-Terms

The potential in momentum space can be written in the partial wave basis as

$$v_{l',l}^{JS}(p', p) = (4\pi)^2 \int_0^\infty dr r^2 j_{l'}(p'r) j_l(pr) V_{l'l}^{JS}(r) \quad (10)$$

Using the Bessel function expansion for small argument $j_l(x) = x^l / (2l+1)!! [1 - x^2/2(2l+3) + \dots]$ we get a low momentum expansion of the potential matrix elements. We keep up to total order $\mathcal{O}(p^4, p^4, p^2 p'^2)$ corresponding to S-, P- and D-waves as well as S-D and P-F mixing parameters,

$$\begin{aligned} v_{00}^{JS}(p', p) &= \tilde{C}_{00}^{JS} + C_{00}^{JS}(p^2 + p'^2) + D_{00}^{1JS}(p^4 + p'^4) \\ &\quad + D_{00}^{2JS} p^2 p'^2 + \dots \\ v_{11}^{JS}(p', p) &= p p' C_{11}^{JS} + p p' (p^2 + p'^2) D_{11}^{JS} + \dots \\ v_{22}^{JS}(p', p) &= p^2 p'^2 D_{22}^{JS} + \dots \\ v_{20}^{JS}(p', p) &= p'^2 C_{20}^{JS} + p'^2 p^2 D_{20}^{1JS} + p'^4 D_{20}^{2JS} + \dots \\ v_{31}^{JS}(p', p) &= p'^3 p D_{31}^{JS} + \dots \end{aligned} \quad (11)$$

We use the spectroscopic notation and normalization of Ref. [30]. The numerical results are shown in Table IV. We see, again, a magnification of errors in the short range contribution due to the lowering of the energy from 350MeV to 125MeV and a confirmation of the universality between OPE and χTPE unveiled in Ref. [16]. Actually we found a correlation pattern which qualifies these counter-terms as good fitting parameters, i.e. small statistical dependence and scheme independence.

TABLE IV: Potential integrals in different partial waves. We separate the contribution from the delta-shells short range parameters (corresponding to $r < r_c = 1.8\text{fm}$) and the χTPE potential tail (corresponding to $r > r_c$). Units are: \tilde{C} 's are in 10^4GeV^{-2} , C 's are in 10^4GeV^{-4} and D 's are in 10^4GeV^{-6} .

	$r < r_c$	$r > r_c$	Full
\tilde{C}_{1S_0}	-0.079(14)	-0.068(1)	-0.15(1)
C_{1S_0}	0.73(8)	3.48(2)	4.20(8)
$D_{1S_0}^1$	-6.2(17)	-440.5(8)	-446.7(19)
$D_{1S_0}^2$	-1.9(5)	-132.1(2)	-134.0(6)
\tilde{C}_{3S_1}	0.051(18)	-0.057(1)	-0.006(19)
C_{3S_1}	-0.078(28)	3.42(2)	3.34(4)
$D_{3S_1}^1$	0.12(4)	-503.7(8)	-503.6(8)
$D_{3S_1}^2$	0.036(13)	-151.1(2)	-151.1(2)
C_{1P_1}	0.54(5)	5.92(4)	6.45(3)
D_{1P_1}	-2.0(2)	-588.8(9)	-590.8(8)
C_{3P_1}	0.79(3)	2.934(8)	3.72(3)
D_{3P_1}	-3.09(9)	-246.1(3)	-249.2(4)
C_{3P_0}	0.046(12)	-4.98(2)	-4.94(1)
D_{3P_0}	0.55(32)	343.7(6)	344.2(5)
C_{3P_2}	-0.221(5)	-0.265(9)	-0.486(8)
D_{3P_2}	0.82(2)	-9.6(4)	-8.8(4)
D_{1D_2}	-0.44(5)	-70.5(1)	-70.9(1)
D_{3D_2}	-2.4(1)	-363.0(2)	-365.4(2)
D_{3D_1}	2.2(3)	202.3(2)	204.5(3)
D_{3D_3}	0.80(11)	-0.13(14)	0.67(16)
C_{E_1}	-1.13(6)	-7.60(2)	-8.72(6)
$D_{E_1}^1$	9.1(9)	998.9(5)	1008.0(8)
$D_{E_1}^2$	3.9(4)	428.1(2)	432.0(3)
D_{E_2}	0.59(7)	82.59(5)	83.18(6)

C. Short distance phase-shifts

A complementary way to visualize the short distance structure of the theory is by looking at the corresponding phase-shifts, δ_l^{Short} , which are those corresponding *just* to the short distance part of the potential $V_{\text{DS}}(r)$ in Eq. (1). Because $V_{\text{DS}}(r)$ has a range of $r_c = 1.8\text{fm}$ the partial wave expansion will converge for $l_{\text{max}} = p r_c$, and so we expect $\delta_{l_{\text{max}+1}^{\text{Short}}} \simeq 0$ within the theoretical uncertainties. In our case $l_{\text{max}} = 2$ which corresponds to D-waves, and so we expect F, G and higher waves to produce negligible phase-shifts from the short distance piece of the potential $V_{\text{DS}}(r)$ in Eq. (1). This is illustrated in Fig. 7, where F and G phase-shifts are very small except for the marginal 3F_3 wave around $\simeq 100$ MeV.

D. Discussion

We see that a feature of our calculation is that a fit up to $T_{\text{LAB}} = 125\text{MeV}$ fulfilling a good $\chi^2/\nu = 1.02$ and passing the normality test requires in addition to the χTPE potential non-vanishing short distance contributions for S, P and D waves, δ_l^{Short} . A way of reducing short distance D-wave phase-shifts is by reducing the value of $l_{\text{max}} = p_{\text{max}} r_c$ to ~ 1 . This can be achieved either by reducing r_c below

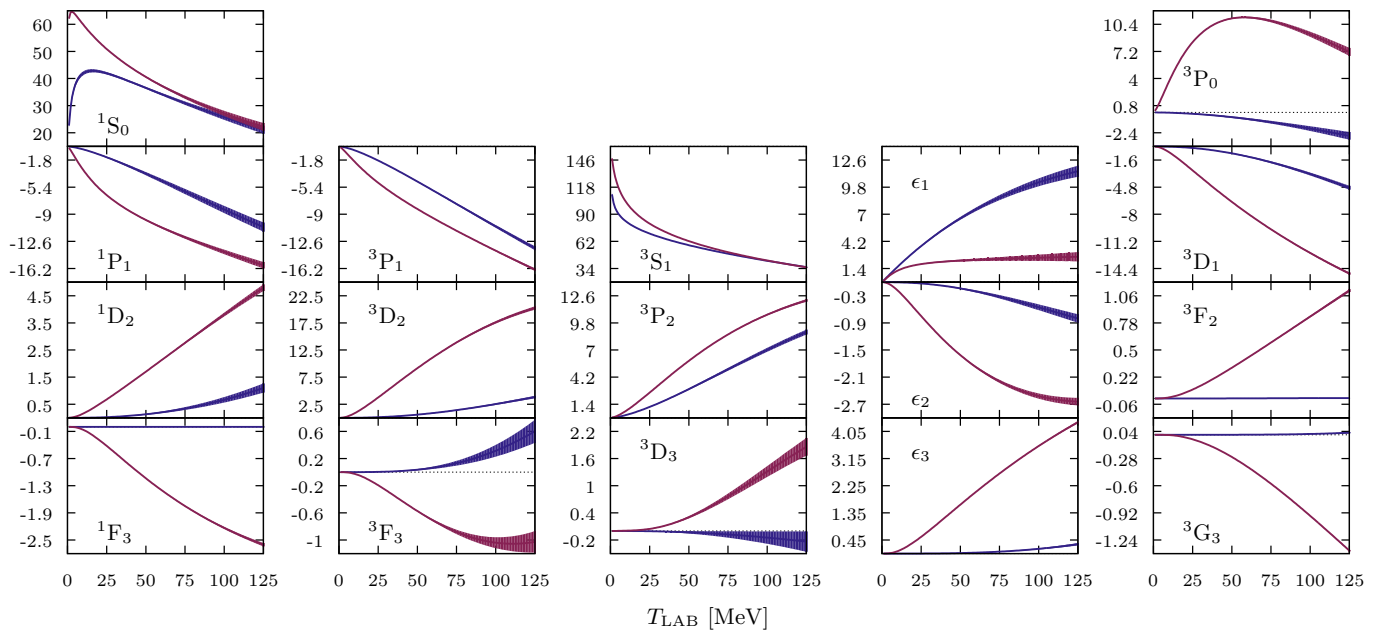


FIG. 7: (Color online) Short distance phase-shifts with statistical error bands in degrees (blue bands) for the δ -shell χ TPE-potential fitted up to a maximum $E_{\text{LAB}} = 125\text{MeV}$ obtained by eliminating all contributions of the potential with $r \geq 1.8\text{fm}$ and keeping just the Delta-shells potential (see main text). The complete phase-shifts (red bands) are drawn for comparison.

1.8fm or p_{max} or both. For instance, choosing $p_{\text{max}} = m_{\pi}$ would correspond to $E_{\text{LAB}} \leq 40\text{MeV}$. Alternatively, one may choose $r_c = 1\text{fm}$ and keep $E_{\text{LAB}} \leq 125\text{MeV}$. According to our discussion on the anatomy of the NN -potential [42] taking $r_c \lesssim 1.8\text{fm}$ the nucleon size and quark exchange effects start playing a role and the elementary particle assumption, upon which the whole NN -potential approach is currently based, gets seriously questioned.

V. COMPARISON WITH OTHER LOW ENERGY CHIRAL POTENTIALS

This work introduces a new phenomenological Nucleon-Nucleon chiral two-pion exchange potential fitted to pp and np scattering data up to a laboratory energy of 125MeV similar in spirit to other recent low energy chiral interactions [32–35] which have become popular in nuclear structure calculations. We comment now on both approaches and the major differences with ours from a statistical point of view.

A. Momentum space optimized chiral potential at NNLO

The momentum space self-denominated optimized chiral nucleon-nucleon interaction at next-to-next-to-leading order potential [32] provides a moderately acceptable $\chi^2/\nu = 1.16$ value. It is based on the 1999 update of the Nijmegen [5, 6] database done with the event of the CD Bonn potential analysis [10] with some minor modifications. With $\nu = N - P = 1945 - 24$ degrees of freedom, one should expect within 68% confidence level a value $\chi^2/\nu = 1 \pm \sqrt{2\nu} = 1 \pm 0.03$, which is

excluded by 5σ ¹. In the standard statistical jargon this means that there is probability $\sim 10^{-7}$ of erring when saying that the distribution *does not* obey a χ^2 distribution. As we have stressed in our previous works[15, 16], one may re-scale a too large χ^2 by a Birge factor to a new $\bar{\chi}^2 = (\chi^2/\chi_{\text{min}}^2)\nu$, which by definition fulfills $\bar{\chi}_{\text{min}}^2/\nu = 1$, *provided* the residuals of the fit are normally distributed. In this case, a re-scaling of experimental uncertainties, namely $\Delta O_i^{\text{exp}} \rightarrow \sqrt{\chi_{\text{min}}^2/\nu} \Delta O_i^{\text{exp}} = \sqrt{1.16} \Delta O_i^{\text{exp}}$, would correspond to a bearable 7% uncertainty in the error (the error of the error). This is the kind of situation (too large χ^2/ν) where the check for normality would be most useful.²

In Ref. [34] the reported skewness and excess kurtosis of the histogram of residuals are $\Delta\mu'_3 = 0.06$ and $\Delta\mu'_4 = 0.37$, respectively. The latter value is a bit too high. Indeed, within a 68% (1σ) confidence level we should have $\Delta\mu'_3 = \sqrt{17/\nu}$ and $\Delta\mu'_4 = 4\sqrt{6/\nu}$, i.e. $\Delta\mu'_3 = 0.09$ and $\Delta\mu'_4 = 0.22$ respectively. The lack of normality is better unveiled in terms of their QQ-plot. They show a line resembling, $Q_{\text{Emp}} \sim 1.35Q_{\text{Th}}$ [34] instead of the expected $Q_{\text{Emp}} \sim Q_{\text{Th}}$ straight line. To better compare with our Fig. 2, that situation is recreated in a rotated QQ-plot in Fig. 8 where the confidence bands are adapted to

¹ Some pp data are excluded in the analysis of [32] on the basis of their extremely high precision which makes the χ^2 value intolerably high. In our case these data are fully included in our 3σ self-consistent database, as we have no obvious reason to discard them.

² Actually, that was the situation we encountered in the χ TPE analysis up to a maximum energy of $E_{\text{LAB}} = 350\text{MeV}$.

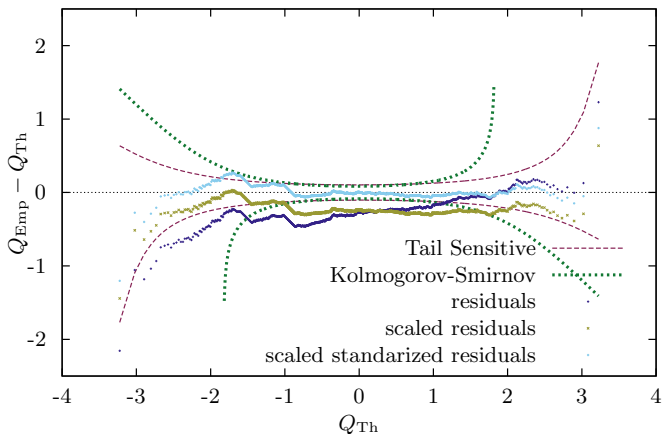


FIG. 8: (Color online) Rotated quantile-quantile plot for the residuals of the low energy optimized momentum space chiral potential of Ref. [34] (dark blue crosses). The scaled (yellow crosses) and standardized (light blue crosses) are also shown. The Kolmogorov-Smirnov (dotted green line) and Tail sensitive (dashed red line) confidence bands with an $\alpha = 0.05$ significance level are also included.

the features of Ref. [34].³

Since in Refs. [32, 34] a different database from our 3σ self-consistent one was adopted, one may think that re-doing the analysis might improve the normality properties of the fit. This is unlikely, because normality requires enough flexibility of the theory to encompass the fitted data up to statistical fluctuations which are tolerated only thanks to the finite number of data. Increasing the database should naturally decrease the fluctuations. In our case, we have $N = 925_{pp} + 1743_{np} = 2688$ data including normalizations vs the $N = 1945$ data used in Refs. [32, 34]. It is unlikely that the bias introduced in the analysis of Refs. [32, 34] will be compensated by *adding* about 700 extra data. Thus, we attribute the lack of normality to a lack of flexibility in the proposed interaction. The question whether our self-consistent database is itself biased by our own analysis is a pertinent one, but this could only be answered by re-doing a data selection anew from scratch. Such an independent data selection analysis would be most welcome to sort out these issues.

B. Local chiral potential

The local chiral potentials [33, 35] fit phase shifts or low energy parameters in the lowest partial waves taken as independent data and provide a sequence of LO, NLO and NNLO schemes. An important feature of this potential concerns the

³ The fact that there appear no points beyond the $Q_{Th} > 3$ and $Q_{Th} < -3$ is due to a truncation in the results shown in Ref. [34]. The total χ^2 obtained for the plot should be $(1848_{\text{data}} + 108_{\text{normalizations}}) \times 1.16 = 2268.96$ while we get 2109.82 for the about 1586 data. A more quantitative analysis computing the p -value would require to totality of data or a truncated gaussian analysis, but will not change the main conclusions from the Fig. 8.

regulator which corresponds to a short distance potential of a range about $1 - 1.2\text{fm}$. We have implemented this potential and checked that their phase-shifts are reproduced for all schemes. We can thus confront this potential to the np and pp database and compute the total χ^2 as a function of the maximal LAB energy. The result is shown in Fig. 9 and as we see the smallest value we get is $\chi^2/N \gtrsim 1$ for $T_{\text{LAB}} \sim 40\text{MeV}$. Nonetheless, our experience in comparing phase-shift with PWA fits suggests that much better values could be achieved with relatively small parameter changes. This is possibly an effect due to the correlations among phase-shifts which in Ref. [33, 35] are certainly ignored. Given their wide applicability in nuclear structure calculations, it would be interesting to perform a full PWA of these local chiral potentials and test their normality.

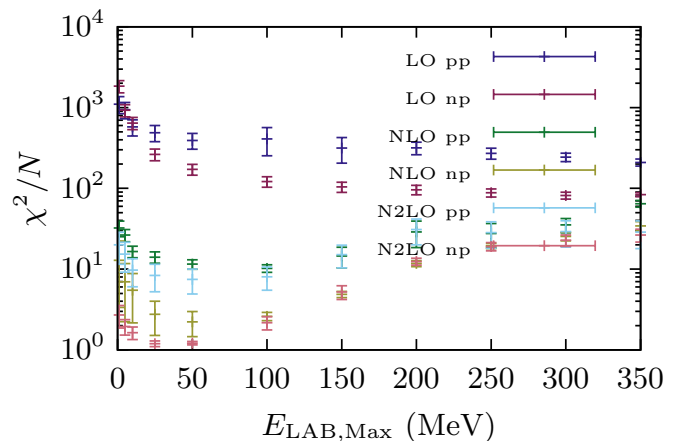


FIG. 9: (Color online) Values of χ^2/N for the local chiral potentials of Ref. [35] as a function of the maximum LAB energy (in MeV). We distinguish the different contributions building their LO, NLO and NNLO for np and pp.

C. Discussion

While the features of both the momentum space and the coordinate space treatments discussed above are different regarding their implementation details and statistical behavior, they share with our present analysis the *same* chiral potential [25] at long distances $r \gtrsim 2\text{fm}$. The main difference relies in the way the short distance pieces of the interaction are represented. As we have mentioned Chiral perturbation theory (χpt) provides a power counting scheme to systematically include pion exchange interactions in the complete NN potential [23, 53]. The several phenomenological chiral potentials which have appeared in the literature include the χpt derived pion exchange for the long range part of the interaction and use counter-terms to describe the *unknown* short range part [28, 29, 32, 35, 54, 55]. However, most of these potentials give a fairly large χ^2/v value when comparing with experimental data. The cases with an acceptable value $\chi^2/v \sim 1$ to data up to 125 MeV [32] the resulting residuals do not follow the standard normal distribution [34]. This lack of normal

residuals could indicate the presence of systematic uncertainties. Since the requirement of normally distributed data is the basic building block of any least squares fit, any resulting theory failing to fulfill this normality condition cannot be trusted as a faithful representation of the scattering data and no reliable propagation of statistical errors can be made. This does not rule out to use them for nuclear structure calculations as it has been done in the past where the normality and error propagation were never addressed. Given this situation, it would be necessary and useful to develop some understanding on how some conservative error estimates could be done when normality is not fulfilled.

However, the main distinct feature which we see is the *necessity of a short distance D-wave component* when we fit up to $E_{\text{LAB}} = 125\text{MeV}$, a feature lacking recent low energy chiral interactions [32–35]. We expect an improvement of normality and quality including these additional terms in their analyzes. We remind that according to the standard power counting invoked in those works the N2LO chiral potential contains, in addition to the longer range OPE and χTPE contributions, just S- and P-wave contact terms, while the contact D-waves should have small contributions. This *a priori* condition is implemented in Refs.[32–35] by choosing a short distance regulator which has a typical range of $r_c \sim 1\text{fm}$. According to our discussion above on short distance phases, this is a way of killing the short distance contribution to the D-waves, since $l_{\text{max}} \sim 1$. Our analysis shows instead a non-vanishing D-wave contribution from the short distance piece of the interaction, within the statistical uncertainties. This fact, while confirms the suitability of the χTPE potential, casts serious doubts on the standard power counting assumed for the short distance components of the interaction. The discussion on the specific power counting to be applied within χPT has been around since the very beginning and most discussions have been carried out on the basis of theoretical consistency [43–45]. Our finding on the D-waves offers an excellent opportunity to discern on the basis of experiment analysis among the several proposals on the market.

VI. CONCLUSIONS

The use of chiral potentials in nuclear physics has become popular in recent years as they are believed to incorporate essential low energy QCD features. While this is formally correct a definite statement supporting this expectation requires to make a decision on whether or not the more than 8000 np and pp available data below pion production threshold are described by the theory with a given confidence level. So far the literature is lacking an estimate of the statistical uncertainties propagated from low energy data only. Such analysis is justified and performed with our new fit. A comparison with other high energy error analyzes allows to evaluate the predictive power of low energy chiral interactions and of course the statistical significance of the included chiral effects.

We have taken the classical statistical point of view of validating the theory using the least squares χ^2 -method. This method rests on the first place on the assumption of normal-

ity of residuals, a question which can be checked a posteriori and is not easy to fulfill. A lack of normality implies the presence of systematic uncertainties in the analysis and excludes propagation of statistical uncertainties.

On the other hand, the available chiral potentials used in current analyzes include OPE and TPE effects which limits the applicability of the theory to about 100 MeV, which is the expected maximum relevant energy for the binding of light nuclei. Thus, we have an interesting opportunity to validate the chiral potential within a statistical analysis of the corresponding low energy data within its range of validity and usefulness for nuclear structure calculations. By using a coarse grained delta-shell representation of the short distance contribution, we observe a good description with an excellent fit. Special attention was given to testing the normality of the residuals which allows to perform a sound propagation of statistical errors. The assumption of normally distributed experimental data was successfully tested. Statistical error quantifications were made for potential parameters, phase-shifts, scattering amplitudes, effective interaction parameters, counter-terms and low energy threshold parameters. In all cases the error bars were considerably larger than the full version of the DS- χTPE potential fitted up to $T_{\text{lab}} = 350\text{MeV}$. This fit also allowed for a new determination of the chiral constants c_1 , c_3 and c_4 compatible with previous determinations from NN and πN data.

Of course, reducing the fitted energy of the fit from 350 MeV to 125 MeV reduces the number of parameters but naturally increases the error bars, not only in the extrapolated energy range, but also in the active fitted range as we have about a third of np and pp scattering data. This is so because the potential intertwines high and low energy scattering data. We find, within uncertainties, unequivocal non-vanishing short distance D-wave contributions to be essential both for the fit and the normality behavior of the residuals. Thus, in order to reduce the strength of the short distance D-wave pieces without becoming sensitive to finite nucleon size details appears to be to lower the maximum fitted energy. A comprehensive and systematic study of such a maximum fitting energy dependence along the lines of our previous study [41] but including normality and uncertainties considerations would be possible and useful but cumbersome and is left for future investigations.

An interesting follow up to this study would be the determination of a low energy potential *without* chiral components with the corresponding statistical error analysis. A comparison of the predictions given by both low energy interactions would show if the inclusion of chiral effect is statistically significant or not, shedding light into the actual predictive power of chiral interactions determined by low energy data only. Some previous results have already been advanced in Ref. [36] suggesting a lack of significance of chiral interactions due to low energy uncertainty enhancement and a more thorough study would be most desirable.

The present work shows that it is possible to fit NN scattering with a Chiral Two Pion Exchange potential fulfilling all necessary statistical requirements up to 125 MeV inferring as a byproduct of the analysis the short distance structure of the

theory. At the same time it offers a unique opportunity to discern, based on a direct comparison to experimental scattering data, on different power counting schemes within the chiral analysis of nuclear forces.

One of us (R.N.P.) thanks James Vary for hospitality at

Ames. We thank Maria Piarulli and Rocco Schiavilla for communications. This work is supported by Spanish DGI (grant FIS2011-24149) and Junta de Andalucía (grant FQM225). R.N.P. is supported by a Mexican CONACYT grant.

-
- [1] H. P. Stapp, T. J. Ypsilantis, and N. Metropolis, *Phys. Rev.* **105**, 302 (1957).
- [2] R. Arndt and M. Macgregor, *Methods in Computational Physics* **6**, 253 (1966).
- [3] R. Machleidt and G.-Q. Li, *Phys.Rept.* **242**, 5 (1994), nucl-th/9301019.
- [4] R. Arndt, W. Briscoe, I. Strakovsky, and R. Workman, *Phys.Rev.* **C76**, 025209 (2007), 0706.2195.
- [5] V. Stoks, R. Kompl, M. Rentmeester, and J. de Swart, *Phys.Rev.* **C48**, 792 (1993).
- [6] V. Stoks, R. Klomp, C. Terheggen, and J. de Swart, *Phys.Rev.* **C49**, 2950 (1994), nucl-th/9406039.
- [7] J. Bergervoet, P. van Campen, W. van der Sanden, and J. J. de Swart, *Phys.Rev.* **C38**, 15 (1988).
- [8] V. G. Stoks, R. Timmermans, and J. de Swart, *Phys.Rev.* **C47**, 512 (1993), nucl-th/9211007.
- [9] R. B. Wiringa, V. Stoks, and R. Schiavilla, *Phys.Rev.* **C51**, 38 (1995), nucl-th/9408016.
- [10] R. Machleidt, *Phys.Rev.* **C63**, 024001 (2001), nucl-th/0006014.
- [11] F. Gross and A. Stadler, *Phys.Rev.* **C78**, 014005 (2008), 0802.1552.
- [12] R. Navarro Pérez, J. E. Amaro, and E. Ruiz Arriola, *Phys.Rev.* **C88**, 024002 (2013), 1304.0895.
- [13] R. Navarro Pérez, J. E. Amaro, and E. Ruiz Arriola, *Phys.Rev.* **C88**, 064002 (2013), 1310.2536.
- [14] R. Navarro Pérez, J. E. Amaro, and E. Ruiz Arriola, *Phys.Rev.* **C89**, 024004 (2014), 1310.6972.
- [15] R. Navarro Pérez, J. E. Amaro, and E. Ruiz Arriola, *Phys.Rev.* **C89**, 064006 (2014), 1404.0314.
- [16] R. Navarro Pérez, J. E. Amaro, and E. Ruiz Arriola (2014), 1406.0625.
- [17] I. Afnan and Y. Tang, *Phys.Rev.* **175**, 1337 (1968).
- [18] R. Navarro Pérez, J. E. Amaro, and E. Ruiz Arriola, *Prog.Part.Nucl.Phys.* **67**, 359 (2012), 1111.4328.
- [19] E. Ruiz Arriola and A. Calle Cordon (2009), 0910.1333.
- [20] A. C. Cordon and E. Ruiz Arriola (2011), 1108.5992.
- [21] S. Aoki (HAL QCD), *Prog.Part.Nucl.Phys.* **66**, 687 (2011), 1107.1284.
- [22] S. Aoki et al. (HAL QCD), *PTEP* **2012**, 01A105 (2012), 1206.5088.
- [23] S. Weinberg, *Phys.Lett.* **B251**, 288 (1990).
- [24] C. Ordonez, L. Ray, and U. van Kolck, *Phys.Rev.Lett.* **72**, 1982 (1994).
- [25] N. Kaiser, R. Brockmann, and W. Weise, *Nucl.Phys.* **A625**, 758 (1997), nucl-th/9706045.
- [26] P. Masjuan, E. Ruiz Arriola, and W. Broniowski, *Phys.Rev.* **D87**, 014005 (2013), 1210.0760.
- [27] T. Ledwig, J. Nieves, A. Pich, E. Ruiz Arriola, and J. Ruiz de Elvira (2014), 1407.3750.
- [28] M. Rentmeester, R. Timmermans, J. L. Friar, and J. de Swart, *Phys.Rev.Lett.* **82**, 4992 (1999), nucl-th/9901054.
- [29] D. Entem and R. Machleidt, *Phys.Rev.* **C68**, 041001 (2003), nucl-th/0304018.
- [30] E. Epelbaum, W. Glockle, and U.-G. Meissner, *Nucl.Phys.* **A747**, 362 (2005), nucl-th/0405048.
- [31] R. Machleidt and D. Entem, *Phys.Rept.* **503**, 1 (2011), 1105.2919.
- [32] A. Ekström, G. Baardsen, C. Forssén, G. Hagen, M. Hjorth-Jensen, et al., *Phys.Rev.Lett.* **110**, 192502 (2013), 1303.4674.
- [33] A. Gezerlis, I. Tews, E. Epelbaum, S. Gandolfi, K. Hebeler, et al., *Phys.Rev.Lett.* **111**, 032501 (2013), 1303.6243.
- [34] A. Ekström, B. Carlsson, K. Wendt, Forssén, M. Hjorth-Jensen, et al. (2014), 1406.6895.
- [35] A. Gezerlis, I. Tews, E. Epelbaum, M. Freunek, S. Gandolfi, et al. (2014), 1406.0454.
- [36] J. E. Amaro, R. Navarro Pérez, and E. Ruiz Arriola, *Few-Body Systems* pp. 1–5 (2013), ISSN 0177-7963, 1310.7456.
- [37] J. Aviles, *Phys.Rev.* **C6**, 1467 (1972).
- [38] D. Entem, E. Ruiz Arriola, M. Pavon Valderrama, and R. Machleidt, *Phys.Rev.* **C77**, 044006 (2008), 0709.2770.
- [39] R. Navarro Pérez, J. E. Amaro, and E. Ruiz Arriola, *Phys.Lett.* **B724**, 138 (2013), 1202.2689.
- [40] R. N. Perez, E. Garrido, J. Amaro, and E. R. Arriola, *Phys.Rev.* **C90**, 047001 (2014), 1407.7784.
- [41] R. Navarro Pérez, J. E. Amaro, and E. Ruiz Arriola, *Few Body Syst.* **54**, 1487 (2013), 1209.6269.
- [42] R. Navarro Pérez, J. E. Amaro, and E. Ruiz Arriola, *Few-Body Systems* pp. 1–5 (2014), ISSN 0177-7963, 1310.8167.
- [43] A. Nogga, R. Timmermans, and U. van Kolck, *Phys.Rev.* **C72**, 054006 (2005), nucl-th/0506005.
- [44] M. P. Valderrama, *Phys.Rev.* **C83**, 024003 (2011), 0912.0699.
- [45] M. Pavon Valderrama, *Phys.Rev.* **C84**, 064002 (2011), 1108.0872.
- [46] S. Aldor-Noiman, L. D. Brown, A. Buja, W. Rolke, and R. A. Stine, *Am. Statist.* **67**, 249 (2013).
- [47] R. Navarro Perez, J. Amaro, and E. Ruiz Arriola, *Phys.Lett.* **B738**, 155 (2014), 1407.3937.
- [48] W. Glöckle, *The quantum mechanical few-body problem* (Springer Berlin, 1983).
- [49] M. Pavon Valderrama and E. Ruiz Arriola, *Phys.Rev.* **C72**, 044007 (2005).
- [50] R. N. Perez, J. Amaro, and E. R. Arriola (2014), 1410.8097.
- [51] M. Moshinsky, *Nuclear Physics* **8**, 19 (1958).
- [52] T. Skyrme, *Nucl.Phys.* **9**, 615 (1959).
- [53] C. Ordonez and U. van Kolck, *Phys.Lett.* **B291**, 459 (1992).
- [54] M. Rentmeester, R. Timmermans, and J. J. de Swart, *Phys.Rev.* **C67**, 044001 (2003), nucl-th/0302080.
- [55] E. Epelbaum, *Prog.Part.Nucl.Phys.* **57**, 654 (2006), nucl-th/0509032.